The mechanics of dunes and antidunes in erodible-bed channels

By JOHN F. KENNEDY

W. M. Keck Laboratory of Hydraulics and Water Resources,
California Institute of Technology†

(Received 6 August 1962 and in revised form 28 February 1963)

An analytic model of free-surface flow over an erodible bed is developed and used to investigate the stability of the fluid-bed interface and the characteristics of the bed features. The model is based on the potential flow over a two-dimensional, moving, wavy bed with a sinusoidal profile of varying amplitude, and a sediment transport relation in which the transport rate is proportional to a power of the fluid velocity at the level of the bed. By assuming that the dominant wavelength is that for which the rate of amplitude growth is the greatest, expressions are obtained for the wavelength and velocity of the bed features. In addition, conditions for the occurrence of the different configurations, dunes, flat bed, and antidunes, are found from the model. The predicted wavelengths of antidunes and ranges of wavelengths of dunes, and the predicted conditions for change of bed configuration are found to be in good agreement with experimental data. Finally, brief consideration is given to the factors involved in determining the maximum heights of the bed features and surface waves.

1. Introduction

Water flowing over an erodible bed of sand interacts with the bed and deforms it into several different configurations. Three principal types of bed features are usually distinguished: dunes, flat bed, and antidunes. These bed forms are the result of an orderly pattern of scour and deposition caused by a systematic perturbation of the gross forward transport of bed material. The nature of the interaction between the bed and fluid and the resulting configuration depend on the depth and velocity of flow, and the properties of the sediment and fluid. For water flowing at a constant depth over a sand bed, the succession of bed configurations with increasing velocity is as follows.

If the flow velocity is great enough to move the individual sand grains but less than another limiting value which will be discussed presently, the bed is spontaneously deformed into irregular features called dunes. A typical dune pattern in a laboratory flume is shown in figure 1, plate 1. The distinguishing features of dunes are: their shape, which in longitudinal section is approximately triangular with a gentle upstream slope that is slightly convex upward and a steep downstream slope; their size and arrangement, which are random for the individual

† Now at Hydrodynamics Laboratory, Department of Civil Engineering, Massachusetts Institute of Technology.

dunes, but uniform in the statistical sense; their downstream movement, which takes place at a rate small compared to the flow velocity; and the flow separation that usually occurs in the lee of the dunes. Dunes are the result of a pattern of scour and deposition due to the perturbation velocities induced by any protuberance on the bed; the dunes themselves are such projections, and are therefore self-propagating. Any small disturbance on an initially flat bed, such as a few sand grains piled above the mean level of the bed, or any external disturbance to the flow, will initiate the growth of dunes if the flow is such that dunes can form. At low Froude numbers the free surface is flat and at higher Froude numbers stationary gravity waves occur that are out of phase with the bed profile. However, a free surface is not essential for the formation of dunes since they also occur in closed conduits carrying sediment-laden flows.

Dunes should be distinguished from the much larger features called sand bars, which have very long, gentle upstream slopes and short, steep downstream slopes. A good description of these bed features has been given by Sundborg (1957). Sand bars are much longer than dunes, and usually occur as isolated features, whereas dunes are periodic and occur in trains. Dunes frequently occur on sand bars.

As the velocity of flow is increased, a value will be reached above which dunes no longer occur, and instead the bed and free surface are flat, as shown in figure 2, plate 2. For this configuration, the fluid-bed interface is stable. If a deformation of the sand bed is artificially induced, it will not persist or propagate, but will decrease in amplitude, and the bed will again become flat. For some depths and sand sizes the flat bed régime does not occur with increasing velocity, and instead sand bars and other bed features that are not of any one well-defined type form after dunes (Simons, Richardson & Albertson 1961).

When the velocity and the Froude number are further increased, the water surface becomes unstable, and even small disturbances give rise to stationary surface waves. The perturbation velocities associated with the surface waves modify the local sediment transport capacity of the flow and thereby cause a pattern of scour and deposition which forms trains of long, sinusoidal-shaped waves of sand that are in phase with the surface waves, and usually move slowly upstream. These features are called antidunes,† and the surface waves accompanying them are referred to as stationary waves or sand waves. A typical antidune configuration in a laboratory flume is shown in figure 3, plate 2. Once initiated, antidunes grow in amplitude until they reach an equilibrium height, or become so high that the surface waves break in the upstream direction. The agitation accompanying wave breaking obliterates the antidunes and levels the bed which then remains flat until another train of antidunes forms. The cycle of wave initiation, growth, and breaking is repeated with a period of one to several

† Sinusoidal-shaped bed features in phase with surface waves were first called antidunes by Gilbert (1914) ' because they are contrasted with dunes in their direction of movement; they travel against the current instead of with it' (p. 31). However, the distinguishing characteristic of antidunes, as the term is used in this paper, is not their direction of movement, but their interaction with surface gravity waves that are in phase with the bed profile. Under this definition, all bed features in phase with surface waves are classed as antidunes, whether they move upstream, downstream, or not at all.

minutes, depending on the depth and velocity of flow and the sand characteristics. Antidunes and the accompanying stationary waves are occasionally three-dimensional (short-crested) in form.

No satisfactory general explanation of the formation and characteristics of the various bed configurations has been proposed. An understanding of the fluid-bed interface is important in river engineering since the roughness of the channel is determined in large part by the form of the bed, and the sediment transport capacity of a flow has been found in laboratory and field studies to be closely related to the bed configuration (Vanoni & Brooks 1957; Simons & Richardson 1961; Tsubaki, Kawasumi & Yasutomi 1953). The purpose of this paper is to present a mathematical model for free-surface flow over an erodible bed, and to use the model to examine the stability of the fluid-bed interface. Expressions for the wavelength and velocity of movement of the bed features are developed, and the conditions under which the various principal bed configurations can occur are investigated. Finally, the maximum heights of the bed features and the waves which form above antidunes are briefly considered. The results of the analysis are compared with experimental data.

2. Free-surface flow over a wavy erodible bed

In this analysis, the forms of the bed and free surface will be idealized as two-dimensional. The flow will be treated as irrotational, and the viscosity, surface tension, and compressibility of the fluid will be neglected. The subscripts x, y, and t denote partial differentiation with respect to the x and y co-ordinates and time, respectively.

Consider the flow over a wavy erodible bed of a fluid with constant mean depth d and flow velocity U in the positive x-direction. Taking the origin of the vertical y co-ordinate, positive upward, at the undisturbed position of the free surface, as shown in figure 4, the profiles of the free surface and bed will be denoted by $y = \xi(x,t)$ and $y = -d+\eta(x,t)$, respectively. The amplitudes of ξ and η will be treated as very small in comparison to the wavelength, and $\partial\xi/\partial x$ and $\partial\eta/\partial x$ will be limited to values very much smaller than unity. With these restrictions, the non-linear terms in the boundary conditions can be neglected. Since the flow is treated as irrotational, the velocity $\bar{q}$ can be expressed as the gradient of a velocity potential ϕ,

$$\bar{q} = (U+u, v) = \nabla\phi,$$

where u and v are the x- and y-components, respectively, of the perturbation velocity due to the waviness of the bed. The incompressibility of the fluid requires that ϕ be harmonic for all t,

$$\nabla^2\phi = \phi_{xx}+\phi_{yy} = 0. \tag{1}$$

The kinematic boundary condition that the velocity at the free surface be tangent to the surface yields

$$U\xi_x+\xi_t = \phi_y \quad \text{on} \quad y = 0. \tag{2}$$

The dynamic condition that the pressure be constant at the free surface is expressed by Bernoulli's equation as

$$g\xi+U\phi_x+\phi_t = 0 \quad \text{on} \quad y = 0. \tag{3}$$

At the interface between the fluid and the bed there are two kinematic conditions to be satisfied. The first is that the velocity component normal to the bed must vanish,

$$U\eta_x + \eta_t = \phi_y \quad \text{on} \quad y = -d. \tag{4}$$

The second condition involves the continuity of sediment movement,

$$G_x + B\eta_t = 0, \tag{5}$$

where $G(x,t)$ is the local rate of sediment transport per unit width on a weight basis (e.g. kilograms per second per metre of width) and B is the bulk specific weight of the sediment in the bed.

For this analysis, the form of the bed will be taken as a sinusoidal wave with varying amplitude,

$$\eta(x,t) = a(t)\sin k(x - U_b t), \tag{6}$$

where $a(t)$ is the amplitude of the bed features, $k = 2\pi/L$ is the wave number, L is the wavelength, and U_b is the velocity of the bed features, assumed constant, in the x-direction (see figure 4). The profile given by (6) is a very good representation of the profiles of antidunes. It is a much poorer representation of dunes which are generally asymmetric. However, because of the separation zones and accompanying free streamlines which occur downstream from the dune crests, as shown in figure 5, (6) appears to be a reasonable approximation for the lowest streamline of flow over dunes. In any event, any bed profile that is a simple harmonic function of x can be obtained by linear superposition of expressions of the form of (6) since it is the most general Fourier component.

The complex potential which satisfies (1) through (4) for the bed profile given by (6) may be obtained in the following way. For a simple harmonic progressive surface wave of fixed amplitude A_0 propagating in the negative x-direction with speed $(U - U_b)$ in a fluid at rest with a horizontal bottom at mean depth D, as shown in figure 4 (*a*), the complex potential is (Milne-Thomson 1960, p. 390)

$$w_0(z',t) = \frac{A_0(U - U_b)}{\sinh kD}\cos k[z' + iD + (U - U_b)t], \tag{7}$$

where $z' = x' + iy'$. The zero subscript will be used to denote quantities pertaining to waves of fixed amplitude. After the co-ordinate transformation $z' = z - Ut$, the co-ordinates are moving with a velocity $-U$ relative to a fixed observer, and the waves are moving with a velocity U_b relative to the co-ordinates. The co-ordinates are then brought to rest by superposing a velocity U on the system; this is accomplished by adding Uz to the complex potential. Since U_b is observed to be always very much smaller than U, it will be neglected compared to U. The resulting flow is shown in figure 4 (*b*). Applying the above operations to (7), the complex potential for slowly moving, fixed-amplitude waves on a fluid flowing with velocity U, as shown in figure 4 (*b*), is

$$w_0(z,t) = Uz + \frac{A_0 U}{\sinh kD}\cos k(z + iD - U_b t). \tag{8}$$

Any streamline can now be replaced by a moving boundary, as shown in figure 4 (*c*). Therefore, (8) is also the complex potential for flow over a slowly moving,

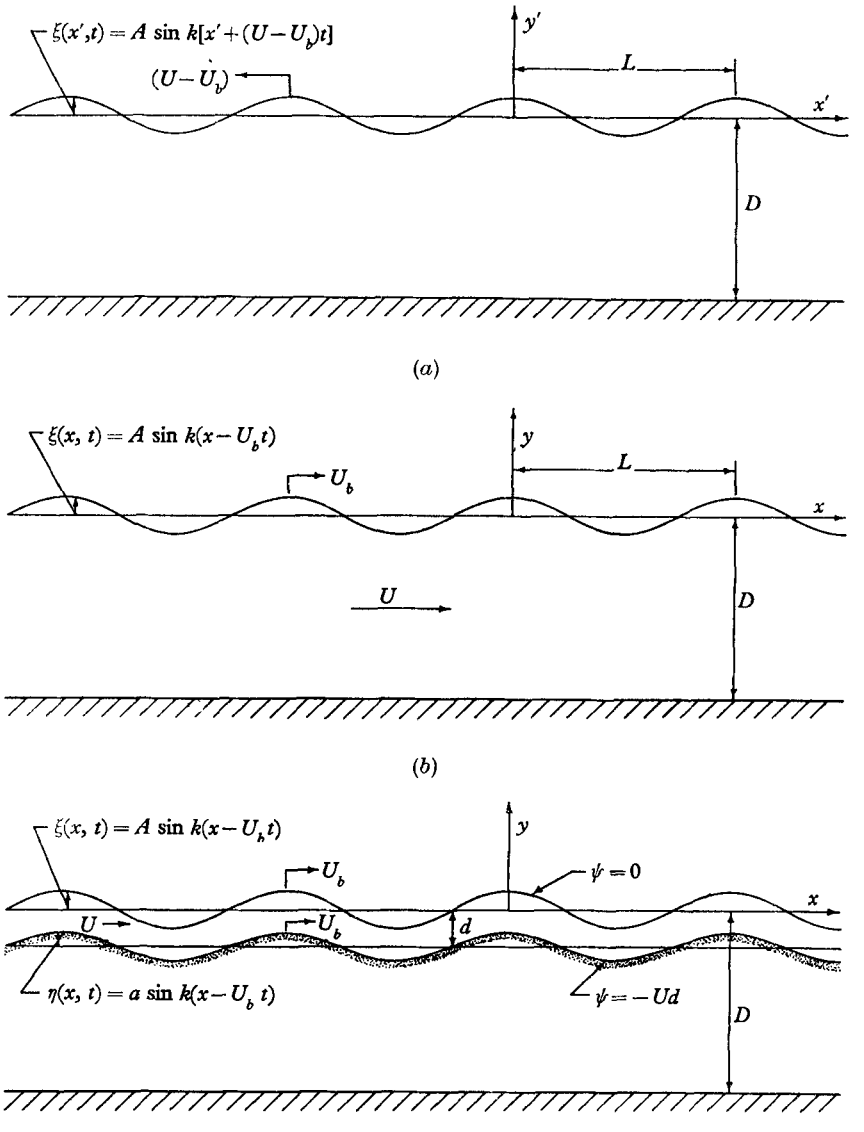

FIGURE 4. Steps in the development of equations for flow over a moving wavy bed. (*a*) Translational gravity waves moving with velocity $-(U - U_b)$ in a fluid at rest with mean depth D. (*b*) Gravity waves moving with velocity U_b in a fluid with a flow velocity U. A velocity U has been superposed on the fluid of figure (*a*). (*c*) Flow over a moving wavy bed. A streamline of the flow shown in figure (*b*) has been replaced by a moving boundary.

wavy bed of fixed amplitude. From the method in which (8) was derived, it is apparent that U, D, and k are related by the usual formula for celerity of waves of small amplitude,

$$U^2 = (g/k) \tanh kD, \tag{9}$$

and the surface profile is given by

$$\xi_0 = A_0 \sin k(x - U_b t). \tag{10}$$

By separating the real and imaginary parts of (8), the velocity potential and stream function can be obtained as

$$\phi_0 = Ux + A_0 U \frac{\cosh k(y+D)}{\sinh kD} \cos k(x - U_b t), \tag{11}$$

$$\psi_0 = Uy + A_0 U \frac{\sinh k(y+D)}{\sinh kD} \sin k(x - U_b t). \tag{12}$$

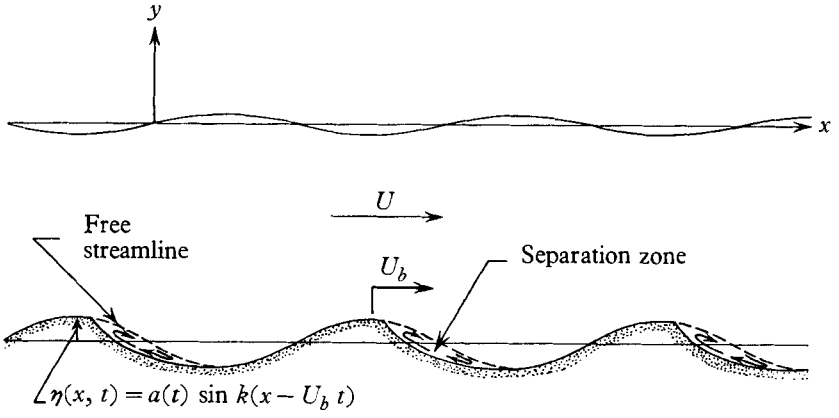

FIGURE 5. Free-surface flow over a dune bed, showing the separation in the lee of each dune. The lowest streamline of the flow is assumed to be a sinusoid.

The bed corresponds to the streamline $\psi_0 = -Ud$ and its position is

$$y = -d + \eta_0(x, t).$$

Substituting these values of ψ and y into (12) and neglecting higher-order quantities yields

$$\eta_0 = A_0 \frac{\sinh k(D-d)}{\sinh kD} \sin k(x - U_b t). \tag{13}$$

The preceding analysis is for flow over a bed of fixed amplitude. However, if A_0 is replaced by $A(t)$ and (10), (11) and (13) are substituted into the boundary conditions given by (2), (3) and (4), it is seen that they are satisfied, provided $A(t)$ is a slowly varying function of t such that $A_t \ll UkA$. Therefore, for flow over a bed of the form given by (6) with slowly varying amplitude the velocity potential is

$$\phi = Ux + UA(t) \frac{\cosh k(y+D)}{\sinh kD} \cos k(x - U_b t), \tag{14}$$

provided $U_b \ll U$. A comparison of (13) and (6) shows that the amplitude of the bed profile is related to the amplitude of the surface waves by

$$a(t) = A(t) \frac{\sinh k(D-d)}{\sinh kD}. \tag{15}$$

Equation (9) can be substituted into (15) with the result

$$a(t) = A(t) \left(1 - \frac{g}{kU^2} \tanh kd\right) \cosh kd. \tag{16}$$

The last two equations show that the bed and water surface profiles are in phase or out of phase according to whether U^2 is greater than or less than $(g/k)\tanh kd$, or equivalently, d is less than or greater than D. For the case in which d is greater than D, the complex potential for the region between the virtual horizontal bottom and the wavy bed (i.e. the region $-d < y < -D$) is the analytical continuation, after an appropriate shift of the origin of vertical co-ordinates, across the horizontal bottom of the complex potential for flow over a wavy bed with $D > d$. The velocity potential ϕ is unchanged and is given by (14).

The remaining boundary condition, (5), will now be used to obtain U_b and $a(t)$. This boundary condition introduces another unknown, the sediment transport rate $G(x,t)$, which necessitates an equation relating G to the other parameters of the flow. Herein lies a stumbling block, for the mechanics of sediment transportation are not at all well understood, and only empirical formulas are available. A modified empirical relation will be used here. It has been observed (Colby 1957; Vanoni & Brooks 1957; Kennedy 1961*b*) that for a given channel and bed material, the sediment transport rate generally increases with the mean flow velocity, and Colby (1961) concludes that the mean velocity is the major factor determining the sediment discharge. Further, in laboratory experiments, Kennedy (1961*a*) found that for a limited range of depth the total sediment transport rate can be expressed as a power of the mean flow velocity. In the present problem, the variation of the local depth of flow over the wavy bed is quite small compared to the mean depth and, in view of the above observations, it seems reasonable to relate $G(x,t)$ to a power of some local velocity. Since the concentration of moving sediment is greatest near the bed, the velocity and the velocity variations in this region have the greatest effect on the local transport rate. Accordingly, the following transport relation will be used

$$G(x,t) = m[\phi_x(x-\delta, -d, t)]^n, \tag{17}$$

where m, n, and δ are constants that depend on the depth and velocity of flow and the properties of the fluid and sediment.

The quantity δ is the distance by which the local sediment transport rate lags the local velocity at the bed, and is included for the following reasons. The transport of sediment by a fluid is due to real-fluid effects; the boundary shear moves the so-called bed load along the bed, and turbulence supports the particles that are swept along above the bed by the flowing fluid. Now if one were to follow a given parcel of fluid, one would expect to observe that, as the fluid velocity decreases (increases), the quantity of sediment transported by the parcel does not immediately decrease (increase) a corresponding amount, since the turbulence intensity and distribution, shear stress in the fluid and on the bed, velocity distribution, and other quantities determining the local sediment transport rate do not change instantaneously as the local depth and local mean velocity change. Instead, at any location, these quantities are strongly influenced by the flow conditions prevailing upstream from this location.† Furthermore, a finite

† The phase shift between the local bed shear stress and the local velocity has been demonstrated theoretically by Brooke Benjamin (1959) for the case of a shearing flow of infinite depth over a wave boundary.

time and corresponding distance are required for the excess entrained sediment to settle to the bed as the velocity and bed shear stress decrease, and for additional sediment to be entrained as the velocity and shear stress increase. It is not now possible, or even consistent in a potential-flow solution, to attempt to take precise account of these real-fluid effects. Instead, only their cumulative effect in causing the local transport rate to lag behind the local velocity is considered, and the quantity δ represents the lag distance. The dependence of δ on the amplitude and wavelength of the bed waves (i.e. on the magnitude and rate of change of the velocity perturbations) is assumed to be negligible, to a first approximation, and δ is considered a function of only the mean depth and velocity of flow and the mobility of the sediment particles in the fluid. This assumption that δ is primarily a property of the undisturbed flow can be valid only for small-amplitude bed features and velocity perturbations, but it appears to be adequate for a linearized wave analysis which itself is valid only for very small amplitudes. The effect of larger bed-wave amplitudes on δ is discussed in § 6.

Expressions for U_b and $a(t)$, the celerity and amplitude of the bed waves, can now be obtained. Substitution of (14) into (17) and expansion into a binomial series yields

$$G(x,t) = mU^n - kmnU^nA(t)\frac{\cosh k(D-d)}{\sinh kD}\sin k(x-\delta-U_bt) + O(u^2). \tag{18}$$

When the higher-order terms in (18) are neglected, the net forward sediment transport rate, $\bar{G}$, for the whole stream at any time is

$$\bar{G} = mU^n. \tag{19}$$

Substitution of (6), (15), (18) and (19) into (5) and neglecting terms of $O(u^2)$ gives the following differential equation for $A(t)$:

$$A_t \sin k(x-U_bt) - A[kU_b\cos k(x-U_bt) + (n\bar{G}k^2/B)\coth k(D-d)\cos k(x-\delta-U_bt)] = 0,$$

the solution to which is

$$A(t) = A(0)\exp\{t(n\bar{G}k^2/B)\coth k(D-d)\sin k\delta - [(n\bar{G}k/BU_b)\coth k(D-d)\cos k\delta + 1]\ln|\sin k(x-U_bt)|\}. \tag{20}$$

Since $A(t)$ is a function of time only, the second term of the exponent of (20) must vanish, giving

$$U_b = -(n\bar{G}k/B)\coth k(D-d)\cos k\delta. \tag{21}$$

Finally, the bed amplitude may be obtained by substituting (20) into (15), and eliminating the x-dependent term by (21):

$$a(t) = A(0)\frac{\sinh k(D-d)}{\sinh kD}\exp\left[t\frac{n\bar{G}k^2}{B}\coth k(D-d)\sin k\delta\right]. \tag{22}$$

Equation (22) shows that the amplitude of small bed waves on an otherwise flat bed caused by any arbitrary disturbance will increase exponentially with time provided k and δ are such that the exponential term in (22) is positive; and

therefore, under these conditions, a flat bed is unstable. The amplitude cannot, of course, continue to grow indefinitely; as the amplitude increases, non-linear effects will arise that govern the equilibrium height of fully developed dunes and antidunes. The nature of these non-linear effects will be discussed in § 6. The expressions for U_b and $a(t)$, (21) and (22), will be examined in §§ 3 and 4 to determine the conditions under which the different bed configurations form, and the characteristics of the bed features.

3. Conditions for occurrence of different configurations

From (15), (21) and (22) five different bed configurations can be distinguished. The various configurations and the conditions for their occurrence are summarized in table 1, and are arrived at as follows.

Case	Bed and surface profiles	$(D-d)$	$k\delta$	$\sin k\delta$	$\cos k\delta$	Movement of bed features	Bed configuration
1	In phase	Positive	$0 < k\delta < \frac{1}{2}\pi$	Positive	Positive	Upstream	Antidunes
2		Positive	$\frac{1}{2}\pi$	Positive	Zero	None	
3		Positive	$\frac{1}{2}\pi < k\delta < \pi$	Positive	Negative	Downstream	
4*a*	No bed waves	Negative	$\pi < k\delta \leqslant \frac{3}{2}\pi$	Negative	Positive	—	Flat bed
4*b*		Negative	$0 < k\delta < \pi$	Positive	—	—	
4*c*		Positive	$\pi < k\delta < 2\pi$	Negative	—	—	
5	Out of phase	Negative	$\frac{3}{2}\pi < k\delta < 2\pi$	Negative	Positive	Downstream	Dunes

TABLE 1. Summary of bed configurations and the conditions for their occurrence.

If the bed and surface profiles are in phase, (15) shows that D is greater than d; then $\coth k(D-d)$ is positive and from (22), $\sin k\delta$ must also be positive if the amplitude of the bed waves is to increase with time. For this case, (21) shows that the bed features will move upstream, remain stationary, or move downstream according as $\cos k\delta$ is positive, zero, or negative. These configurations correspond to cases 1, 2 and 3, respectively, in table 1.

Similarly, for D less than d, (22) shows that $\sin k\delta$ must be negative for the features to grow and thus $k\delta$ must be between π and 2π. From (21), it is seen that the bed features will move upstream if $\pi < k\delta < \frac{3}{2}\pi$, remain stationary if $k\delta = \frac{3}{2}\pi$, and move downstream if $\frac{3}{2}\pi < k\delta < 2\pi$. However, it appears that the first two of these configurations are not possible, due to the following real-fluid effect. When the bed and surface profiles are out of phase, an adverse pressure gradient occurs on the downstream slopes of the bed features and produces flow separation in the lee of each dune, as shown in figure 5. As the particles moving along and near the bed pass over a dune crest, some of them settle out of the main flow into the separation zone and are deposited on the bed; this deposition on the lee-slopes of the dunes causes the dunes to move downstream. Now an upstream movement would require the occurrence of scour on the downstream slopes in the regions of flow separation and deposition on the upstream slopes where the lowest streamline is in contact with the bed. Similarly, stationary dunes could occur only if there were no net deposition in the lee of the dune crests. These two patterns of scour and deposition do not seem physically possible, and have not, in fact, been observed in the laboratory or in natural streams.

Therefore, if $D < d$ and $\pi < k\delta \leqslant \frac{3}{2}\pi$, the only admissible solution is the trivial one, $a(t) = 0$, corresponding to the flat bed. This condition is represented in table 1 by case 4*a*. Case 4 also includes the situation in which $(D-d)$ and $\sin k\delta$ are different in sign, giving a negative exponent in (22) so that $a(t)$ decreases with time and the bed becomes flat.

Case 5 represents the configuration for the bed and surface profiles out of phase and $\frac{3}{2}\pi < k\delta < 2\pi$, giving a downstream movement of the features.

An interesting observation in table 1 is that as the velocity is increased (with d held constant, say) so that the bed form changes from dunes to flat bed to antidunes, $k\delta$ decreases from a value greater than $\frac{3}{2}\pi$ to less than $\frac{1}{2}\pi$ (excluding the flat bed corresponding to $(D-d)$ and $\sin k\delta$ being different in sign). It is experimentally observed (for example, Kennedy 1961*a*; Brooks 1954) that L generally increases with U. Thus, the decrease in $k\delta$ indicates that with increasing U, δ increases less rapidly than L (or possibly even decreases).

A meaningful distinction between dunes and antidunes is that antidunes are any features for which $D > d$, while for dunes, $D < d$. Using this criterion, antidunes occur only at relatively high velocities (large values of D and, from (9), large U for a given k) and the antidune régime is separated from the dune régime by the flat-bed régime as $k\delta$ varies with changing flow conditions. According to this criterion, cases 1, 2, and 3 of table 1 represent antidunes. Case 1 represents antidunes that move upstream; this is the most frequently observed type in both natural and laboratory streams. Antidunes that remain stationary and antidunes that move downstream, cases 2 and 3, have been observed in laboratory flumes (Kennedy 1961*a*; Simons *et al.* 1961). Case 5 represents the ordinary type of dunes, which always move downstream.

It should be noted that although frequent mention is made herein of free-surface waves accompanying dunes, the amplitude of these waves may be so small that they are not readily observed. For example, typical parameters for a dune configuration and the accompanying flow might be $kd = 5{\cdot}0$ and $F = 0{\cdot}4$, where $F^2 = U^2/gd$. For these values, (16) yields $A/a = 0{\cdot}054$, so the surface-wave amplitude is less than 6 % of the dune amplitude. For longer dunes, the surface wave can actually be observed, as described by Simons *et al.* (1961).

4. Wavelength and velocity of movement of bed features

Thus far the wavelength, L, has been left arbitrary, the only restriction being that the flow velocity U, the depth D to the virtual horizontal bottom, and the wave-number k are related by (9). Therefore, L can take on any value greater than the minimum, L_m, given by

$$L_m = 2\pi U^2/g, \tag{23}$$

which (9) yields for $D \to \infty$. However, in both natural and laboratory streams, it is observed that for each flow velocity, depth, and bed material, there is a characteristic wavelength that is dominant over all others. It is shown in this section that the dominant wavelength can be predicted from the model developed in § 2. When the wavelength is known, the type of bed configuration and velocity of the bed features can also be determined.

Proceeding in the usual manner of fluid-stability analysis, it is assumed that the dominant wavelength is that for which the initial rate of growth given by the linearized formulation is the greatest (see Brooke Benjamin 1957 for a discussion of the logic of this method of analysis). The problem now consists of determining the value of k for which a_t is a maximum at $t = 0$. From (22), the initial rate of growth is

$$a_t(0) = A(0)\frac{n\bar{G}k^2}{B}\frac{\cosh k(D-d)}{\sinh kD}\sin k\delta. \tag{24}$$

The wave-number of the dominant wavelength is obtained by differentiating (24) with respect to k and equating the resulting expression to zero. Thus, after eliminating D by (9), the dominant wavelength is the solution to

$$\frac{da_t(0)}{dk} = A(0)\frac{n\bar{G}}{B}\left\{[2k\sin k\delta + k^2\delta\cos k\delta]\left[\frac{g}{kU^2}\cosh kd - \sinh kd\right]\right.$$
$$\left. + k^2\sin k\delta\left[-\frac{g}{k^2U^2}\cosh kd + \frac{gd}{kU^2}\sinh kd - d\cosh kd\right]\right\} = 0,$$

which can be rearranged to yield

$$F^2 = \frac{U^2}{gd} = \frac{1 + kd\tanh kd + k\delta\cot k\delta}{(kd)^2 + (2 + k\delta\cot k\delta)\,kd\tanh kd}, \tag{25}$$

where F is the Froude number of the flow. It is expedient to express (25) in terms of F, the dimensionless product kd, and a dimensionless quantity relating the lag distance to the flow depth. This is accomplished by letting $\delta = jd$, where j is a dimensionless quantity that depends on the depth and velocity of flow and the fluid and sediment properties. Substituting this expression for δ into (25) results in

$$F^2 = \frac{1 + kd\tanh kd + jkd\cot jkd}{(kd)^2 + (2 + jkd\cot jkd)\,kd\tanh kd}. \tag{26}$$

Equation (26) relates the wave number of the dominant wavelength to the parameters of the flow, F and d, and j, which represents the properties of the fluid and bed material.

A limiting case of (26) of particular interest is that for which $\delta \ll d$. This case is obtained by letting $j \to 0$ in (26):

$$\lim_{j\to 0} F^2 = \frac{2 + kd\tanh kd}{(kd)^2 + 3kd\tanh kd}. \tag{27}$$

This expression will be useful for comparing the relations given by (26) for different values of j.

The velocity, U_b, of the bed features of the dominant wavelength can be obtained by first using (9) to eliminate U^2 from (26) and then using the resulting expression to eliminate D from (21). The result, after some simplification, is

$$U_b = \frac{n\bar{G}k}{2B}\left[\frac{\sinh 2kd + 2kd}{\sinh^2 kd - jkd\cot jkd - 1}\right]\cos jkd. \tag{28}$$

In the limiting case $j \to 0$, for which the wavelength is given by (27), U_b is

$$\lim_{j\to 0} U_b = \frac{n\bar{G}k}{2B}\left[\frac{\sinh 2kd + 2kd}{\sinh^2 kd - 2}\right]. \tag{29}$$

Figure 6 shows the relation between F and kd given by (26) for values of j of 0·5 and 2, and for the limiting case $j = 0$ given by (27). In addition, the relation between F and kd for the shortest two-dimensional (long-crested) waves that can form is shown. This relation is obtained by dividing (23), which gives the length of the shortest possible two-dimensional waves, by $2\pi d$ with the result

$$F_m^2 = L_m/2\pi d = 1/kd, \tag{30}$$

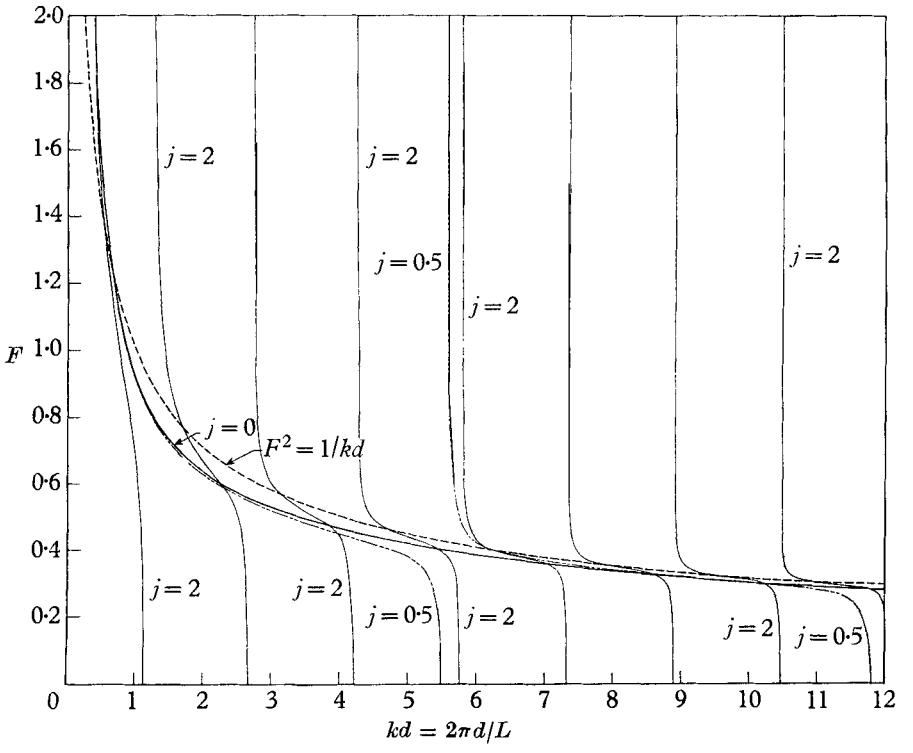

FIGURE 6. Variation of Froude number with kd given by (26) for values of j of 0, 0·5, and 2. The (F, kd)-relation for the shortest possible two-dimensional waves, $F_m = (kd)^{-\frac{1}{2}}$, is also shown.

where F_m is the maximum possible Froude number for a given k and d if the waves and bed features are two-dimensional. Thus, for long-crested waves, kd can take on any value between zero and $1/F^2$; only if three-dimensional (short-crested) waves form can kd exceed this value, since for any U and D these waves are shorter than two-dimensional waves (Fuchs 1952). Therefore, in the region of figure 6 to the right of the curve $F = F_m = (kd)^{-\frac{1}{2}}$, only three-dimensional waves can form and their wavelength is not given by (26), which was derived for long-crested waves. The reason that (26) predicts values of kd larger than the maximum permissible for long-crested features in some ranges of F and j is that, in these ranges, the maxima and minima of a_l as a function of kd, whose loci are given by (26), occur at values of kd exceeding $1/F^2$. Stated another way, for some values of F and j, (26) has some roots that exceed $1/F^2$, and these roots

are not admissible because they would require values of $\tanh kD$ greater than unity in (9).

For each value of j other than zero, (26) is seen to have an infinite number of singularities, one at each value of kd for which the denominator is zero. These singularities occur at negative values of $\cot jkd$, since all other terms in the denominator are positive. Now $\cot jkd$ is periodic with a period of π, and takes on all real values from $+\infty$ to $-\infty$ in each period. Therefore, (26) has one singularity in each π-interval of jkd, and the singularities separate the different branches of the equation. In figure 6, the singularities appear as discontinuities where F jumps from zero to plus infinity.† It is noteworthy that in regions away from their singularities, the relations for the different values of j are grouped closely around the curve for the limiting case $j = 0$. This is the reason it is convenient to use this relation as a reference curve; it also has the desirable properties of being single-valued and continuous for all positive values of kd.

Of the infinite number of branches of (26) for each j, only the first two and part of the third are of interest, the branches for the larger values of kd being inadmissible for the following reason. If jkd is greater than 2π, then L is less than δ. If this were the case, it would mean that the wavelength which developed was such that the material entrained at any point would be carried completely over the bed feature downstream from the one where it had resided, and deposited on the second feature downstream. Now the local velocity, bed shear stress, turbulence, and other factors responsible for the sediment transport are periodic with period L, and hence it does not seem reasonable that the local sediment transport at any point should be influenced by conditions a distance greater than L upstream. Consequently, the relation for each j has physical significance only where L is greater than δ, or equivalently, on the portions of the curves where jkd is less than 2π. This includes only the first two branches and a part of the third.

The values of kd and corresponding values of F for the formation of each of the bed configurations given in table 1 can now be determined for any j. These are shown for several different j's in figure 7 on curves representing (26) similar to those shown in figure 6. Two supplementary equations, (30) and a special form of (9), that will facilitate the discussion of this figure are also included in the graph. This rather complicated figure calls for a detailed explanation, as follows.

The first supplementary equation shown in figure 7 is $F = F_m = (kd)^{-\frac{1}{2}}$; this is the (F, kd)-relation for $D = \infty$. Long-crested waves are not a possible configuration in the region above this curve, as discussed previously. The other equation shown is the (F, kd)-relation for the special case $D = d$. This is obtained by replacing D by d in (9) and dividing by gd with the result

$$F_a^2 = \tanh kd/kd, \tag{31}$$

where F_a, as will be seen presently, is the minimum F for the formation of antidunes. This is the relation that must hold for all values of j if the virtual hori-

† Actually, F changes from $i\infty$ to ∞, since F^2 goes from $-\infty$ to $+\infty$; however, only real positive values of F are shown because other values have no physical significance.

zontal bottom is at the level of the actual channel bed.† For a given kd, F will be greater than or less than F_a according as $D > d$ or $D < d$.‡ In table 1, it is seen that D is greater than d for antidunes and less than d for dunes, and consequently, antidunes occur only in the region above this curve. Thus, for any kd, F_a given by (31) is the minimum F for the formation of antidunes, and the maximum F for the formation of dunes.

The (F, kd)-relations given by (26) are not shown in the regions of figure 7 where $jkd > 2\pi$ or where $F > F_m$. In the first of these instances, (26) has no physical significance, since δ is greater than L, and in the second, it is not the appropriate wavelength relation since two-dimensional waves cannot form. Thus, the first branch shown for each j does not extend above the curve $F = F_m$, and none of the third branch is included, since the portion of it which is of interest, $jkd < 2\pi$, lies entirely above $F = F_m$. In addition, for each j the segment of the first branch that lies below $F = F_a$ is not shown for the following reason. In this region, $D < d$ and $jkd < \pi$, and hence the exponent of (22) is negative, so the amplitude of the bed waves diminishes with time, giving a flat bed. This corresponds to case 4*b* in table 1. In fact, these portions of the first branches are the (F, kd)-relations for which the rate of amplitude decrease is a maximum. Since the bed configuration is fully defined by the branches for which the bed features grow, the inclusion of these segments for diminishing amplitude would serve no purpose.

For each value of j other than zero in figure 7, the intervals over which antidunes moving upstream, antidunes moving downstream, and dunes occur are shown by broken lines, short-dashed lines, and solid lines, respectively, on the curves representing (26). In the intervals where a flat bed is predicted by table 1, the (F, kd)-relations given by (26) are shown by long-dashed lines; actually, in these ranges of F, dunes can form, but their wavelength cannot be predicted with the present model, as will be discussed below along with the significance of the short vertical line segments. The bounds of the different intervals are deduced in the following way. As explained in § 3 and shown in table 1, antidunes form only if $D > d$, and move upstream if $0 < jkd < \frac{1}{2}\pi$, and downstream if $\frac{1}{2}\pi < jkd < \pi$. It follows then that antidunes occur in the region of figure 7 above the curve $F = F_a$ (F_a being the Froude number for $D = d$) and their direction of movement changes at $jkd = \frac{1}{2}\pi$. For the dune configuration, table 1 (case 5) shows that $D < d$ and hence, this bed form occurs below the curve $F = F_a$ in the intervals where $\frac{3}{2}\pi < jkd < 2\pi$. In the range of Froude numbers between where the first branch of the (F, kd)-relation for any j intersects the $F = F_a$ curve from above and the vertical line segment for that j intersects the $F = F_a$ curve from below, the only admissible solution for two-dimensional features is the trivial one, the flat bed.

† If the bottoms do coincide, (15) shows that the surface-wave amplitude A can be finite only if the bed waves have zero amplitude. Then the formulation presented in § 2 reduces to that for a stationary surface wave in a channel with a horizontal bottom.

‡ This can be reasoned as follows. If $D = d$, the virtual and actual channel bottoms coincide and $F = F_a$. Equation (9) shows that U, and hence F, is a monotonically increasing function of D for fixed k. Therefore, $F \gtrless F_a$ according as $D \gtrless d$.

There are two regions of figure 7 in which the bed configuration is not uniquely defined by the present two-dimensional, maximum-rate-of-growth model. The first of these regions is that in which a flat bed is predicted by table 1 (case 4*a*), i.e. the region where $D < d$ and $\pi < jkd < \frac{3}{2}\pi$, and in which the (F, kd)-relations are shown by long-dashed lines in figure 7. For any j, the area below the curve $F = F_a$ and to the right of the vertical line segment extending upward from the

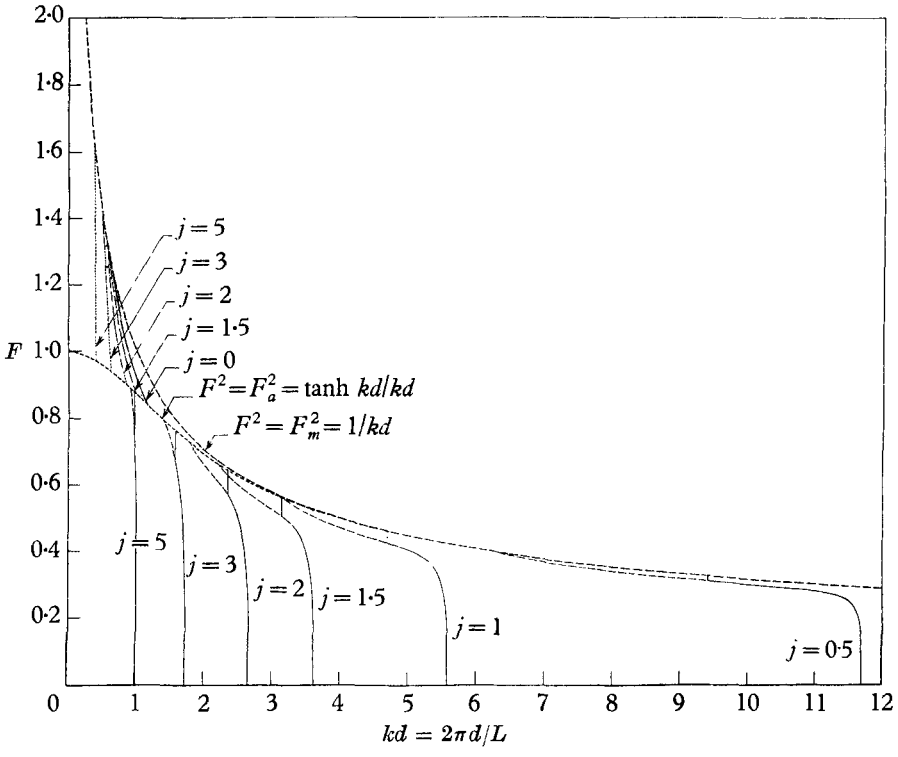

FIGURE 7. Regions of occurrence of different bed configurations for several values of j. $F = F_a$ is the minimum Froude number for the occurrence of antidunes, and the maximum Froude number for the occurrence of dunes. $F = F_m$ is the maximum Froude number for the occurrence of long-crested features. The different configurations are denoted by the character of the lines representing (26) (except for $j = 0$), as follows: —·—, antidunes moving upstream; - - - -, antidunes moving downstream; ——, dunes; – – – –, region in which flat bed is predicted by table 1. The short vertical line segments show for each j the range of F over which the régime of transition from dunes to flat bed occurs. The flat bed is the configuration for Froude numbers between the transition régime and antidune régime.

(F, kd)-relation (26) at $jkd = \frac{3}{2}\pi$ fulfils the requisites for dune formation. (Note that, in the area to the left of this vertical line segment, dunes are not a possible configuration because $jkd < \frac{3}{2}\pi$ for the j in question; however, this is an area of possible dune formation for a larger j, and hence the whole region between the curve $jkd = \frac{3}{2}\pi$ (not shown) and the curve $F = F_a$ is a region where dunes can form.) For Froude numbers in this range, dunes can form, but their wavelength is not given by (26). If it is assumed that the wavelength with the maximum

initial growth rate dominates, then the wavelength is given by $jkd = \frac{3}{2}\pi$;† however, as discussed in § 3, dunes with $jkd = \frac{3}{2}\pi$ cannot form because their existence would require no net deposition on the downstream slopes in the region of separation, and no scour on the upstream slopes. Thus, there is a region of transition from dunes to flat bed in which the bed configuration is not completely described by this analysis. For any j, the lower Froude number for this transition region is the F corresponding to $jkd = \frac{3}{2}\pi$, and the upper Froude number is the F at the intersection of the curve $F = F_a$ and the vertical line extending from the point $jkd = \frac{3}{2}\pi$. It is noteworthy that in laboratory experiments the change in bed configuration from dunes to flat bed does not occur at a sharply delineated set of flow conditions; instead, there is a range of Froude number for any depth in which the bed configuration does not consist of features of any one well-defined type. Vanoni & Brooks (1957) observed alternate reaches of dunes and flat bed for these intermediate Froude numbers. Simons *et al.* (1961) have termed this the 'transition régime' because the bed features are so varied, and are dependent not only on the depth and velocity of flow, but also on the form of the bed before the flow was started. They observed that the bed form in the transition régime was 'in between dunes and a plane bed and consisted of washed out dunes and sand bars' (p. A-47).

The other region in which the configuration is not uniquely defined is that above the curve $F = F_m$. In this region, only short-crested features can form and are not described by the model developed here for two-dimensional waves. However, the experimental data presented in § 5 and shown in figure 9 generally lie below the curve $F = F_m$, the only exception being antidunes at higher Froude numbers, which agree well with the (F, kd)-relation for $j = 0$, equation (27). In laboratory experiments, Kennedy (1961*a*) found that the wavelengths and behaviour of short-crested and long-crested antidunes were not significantly different. Therefore, as a practical matter, the failure of the present model to describe three-dimensional waves and bed features is not a severe limitation.

The regions delineated by the character of the lines in figure 7 for the occurrence of the different bed configurations are shown in figure 8 in the (F, j)-plane. Several interesting observations can be made from this figure. First, there is a minimum F, that occurs at $j = 0$, for the change in bed form from flat bed to antidunes. An expression for the value of kd at which this change in bed form occurs (the kd at which the (F, kd)-relation given by (26) for any j intersects the $F = F_a$ curve in figure 7) can be obtained by substituting the expression for F_a given by (31) for F in (26). The value of kd for the intersection of these curves is found to be the solution to

$$\sinh^2 kd - jkd \cot jkd = 1. \tag{32}$$

† That this vertical line segment represents dunes with the maximum growth rate can be reasoned in the following way. On the successive branches of (26) da_t/dk and $da_t/d(kd)$ for constant d, is alternately a maximum and a minimum. Therefore, between any branch where a_t is a maximum and the next branch to the right, a_t is a monotonically decreasing function of kd for any constant F. Hence, a_t will be a maximum for the smallest admissible values of kd in the region. For the situation in question, this is the vertical line segment $jkd = \frac{3}{2}\pi$.

For $j = 0$, (32) reduces to $kd = \sinh^{-1}\sqrt{2} = 1{\cdot}147$ and the corresponding F given by (27) is $F = F_a = 0{\cdot}844$. This is the lowest possible Froude number for the transformation from flat bed to two-dimensional antidunes. In figure 7 it is obvious that the highest possible F for this change is unity.

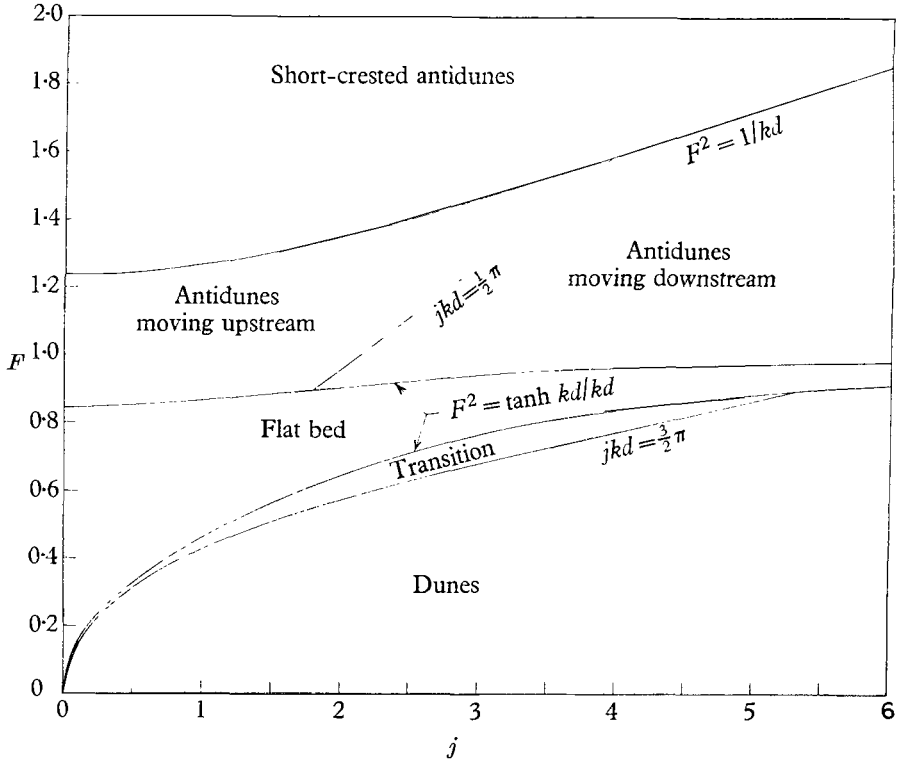

FIGURE 8. Conditions for occurrence of different bed configurations.

Another significant point shown in figure 8 is that for small values of j, antidunes moving downstream cannot occur. The conditions for the absence of these bed features is that the point at which $jkd = \frac{1}{2}\pi$ on the (F, kd)-relation given by (26) falls below the curve $F = F_a$ (given by (31)) in figure 7. Therefore, the minimum value of j at which these antidunes can occur is obtained by substituting $jkd = \frac{1}{2}\pi$ (the value of jkd at which the direction of antidune movement changes, as shown in table 1) into (32), which gives the intersection of (26) and (31), with the result $kd = \sinh^{-1} 1 = 0{\cdot}881$. Substituting this value of kd into $jkd = \frac{1}{2}\pi$ yields $j = 1{\cdot}78$. For smaller j the only antidunes possible are those that move upstream. It is also apparent in figure 8 that two-dimensional antidunes moving upstream are not a possible configuration at large values of j. The maximum j for the occurrence of these antidunes is obtained by substituting $F^2 = 1/kd$ into (26) and letting $jkd = \frac{1}{2}\pi$. This results in

$$kd + 2\tanh kd = 1 + kd\tanh kd,$$

which has the solution $kd = 0{\cdot}396$. Substituting this kd into $jkd = \frac{1}{2}\pi$ gives $j = 3{\cdot}97$. For larger j, two-dimensional antidunes moving upstream cannot form.

The régime of transition is the region of figure 7 above the curve $jkd = \frac{3}{2}\pi$ (not shown) and below $F = F_a$. Therefore, for any values of j such that the point on the (F, kd)-relation where $jkd = \frac{3}{2}\pi$ lies above $F = F_a$, the transition régime does not occur. In figure 8 it can be seen that this is the situation at higher values of j. The maximum j for the occurrence of the transition régime can be obtained by substituting $jkd = \frac{3}{2}\pi$ into (32) with the result $kd = \sinh^{-1} 1 = 0{\cdot}881$. When this value of kd is substituted into $jkd = \frac{3}{2}\pi$, the result is $j = 5{\cdot}35$. The transition régime does not occur for larger j.

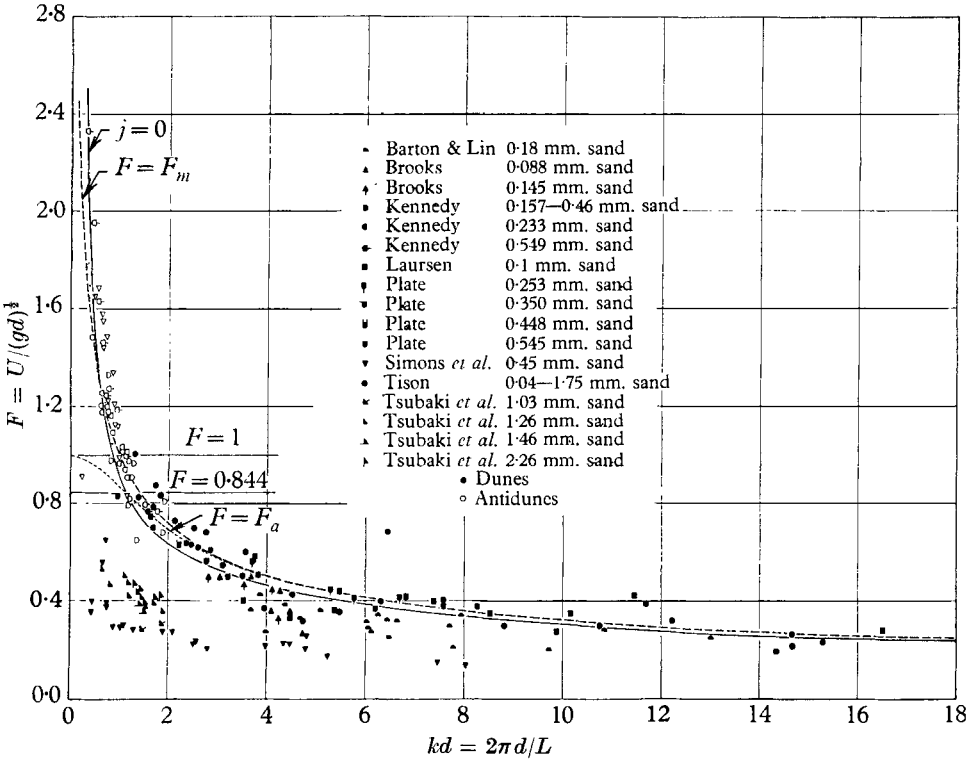

FIGURE 9. Comparison of predicted and observed regions for formation of different bed configurations.

5. Comparison with experimental data

Figure 9 shows a comparison of experimental data reported by various investigators and the reference curves shown in figures 6 and 7. The reference curves are the (F, kd)-relation for $j = 0$, (27); the maximum possible Froude number for long-crested features, (30); and the minimum Froude number for antidunes and maximum for dunes, (31). In addition, the minimum and maximum Froude numbers for the change in bed form from flat bed to antidunes ($F = 0{\cdot}844$ and 1) are delineated. The sources of the data and a brief summary of the range of variables represented are given in table 2. In figure 9 the bed configuration is noted by the shading of each point. Since there is little consistency in the terminology used to describe bed features, and some authors did not

include a description of the bed profile, the noted configurations represent the present writer's classification based on the investigators' descriptions of the bed. For Tison's data, all bed forms are plotted as dunes, and for the natural stream data reported by Kennedy, all bed forms are plotted as antidunes, since it was not possible to distinguish between dunes and antidunes for these two sets of data.

Source	Description of stream	Range of depth (cm)	Range of velocity (cm/sec)	Median sand size (mm)
Barton & Lin (1955)	Lab. flume	9·1 – 42·1	21·6– 53·3	0·18
Brooks (1954)	Lab. flume	5·70– 8·66	25·0– 40·8	0·088
		6·00– 9·1	28·3– 42·7	0·145
Kennedy (1961*a*)	Lab. flume	4·42– 10·61	47·9–105·2	0·233
	Lab. flume	3·75– 10·55	50·3–141·7	0·549
	Natural streams	5·5–120	64 –244	0·157–0·46
Laursen (1957)	Lab. flume	7·62– 30·33	32·6– 70·4	0·1
Plate (1957)	Lab. flume	2·86– 5·55	30·2– 33·2	0·253
		1·31	2·9	0·350
		3·02	34·2	0·448
		3·44– 11·98	37·2– 41·1	0·545
Simons *et al.* (1961)	Lab. flume	5·88– 30·36	21·3–188·4	0·45
Tison (1949)	Lab. flume	1 – 34	18 – 50	0·04–1·75
Tsubaki *et al.* (1953)	Irrigation canals	30·9 – 36·1	53·3– 53·6	1·03
		10·8 – 46·7	54·9– 76·5	1·26
		29·5 – 35·9	66·1– 74·0	1·46
		25·2 – 32·9	73·0– 77·5	2·26

TABLE 2. Summary of range of variables represented by data of figure 9.

For the higher Froude numbers, in the antidune régime, the experimental points are grouped closely around the theoretical relation for $j = 0$, (27). Since the relations for other values of j converge to (27) for these larger values of F, as can be seen in figure 6, the agreement with theory is quite good in this region. It is actually somewhat surprising that the agreement with (27) is so good at the high values of F (greater than 1·24) where it predicts values of kd greater than the maximum possible for long-crested features, (30). In the dune régime (F smaller than about 0·8) practically all points fall below the curve, giving the theoretical maximum Froude number for dunes, $F = F_a$. Note also that antidunes generally occur in or above the predicted range of minimum Froude number for their formation, $F = 0{\cdot}844$ to 1. Thus, for the whole range of F and kd, figure 9 indicates good agreement between theory and experiment.

There is no means of showing in figure 9 experimental data for flows producing a flat bed. However, the data (unpublished) on the wavelengths of the dunes for the constant-depth experiments by Vanoni & Brooks (1957) and the constant-discharge experiments by Kennedy (1961*b*) show that the dune régime does end at or very near the predicted maximum, $F = F_a$. The experimental data of Simons & Richardson (1961), and the data from the experiments by Kennedy

(1961*a*) at high values of F indicate that the transition from flat bed to antidunes occurs in the predicted range ($F = 0{\cdot}844$ to 1).

In figure 8, it can be seen that for large values of j the flat-bed régime occurs only over a narrow range of Froude numbers. For example, with $j = 5$ the régime of transition from dunes to flat bed ends at $F = 0{\cdot}88$, and the change from flat bed to antidunes occurs at $F = 0{\cdot}97$. Moreover, the range of F for the flat bed decreases with increasing j; therefore, if j increases as F is increased, the range of F for the flat bed will be further reduced. In the experiments of Simons *et al.* (1961) shown in figure 9, which for F above about 0·4 have large values of j as can be seen by plotting these points on figure 7, no runs with a flat bed were obtained between the dune and antidune régimes. Apparently in these experiments the variation of j with F was such that the flat-bed régime could not occur.

6. Maximum heights of bed features and surface waves

Both dunes and antidunes are observed to have maximum heights, which depend on the depth and velocity of flow and the properties of the fluid and sediment. As with the wavelengths, the maximum height is quite uniform for the antidunes of a given flow, but variable for the individual dunes. The linearized analysis developed in § 2 cannot, of course, be used to predict the maximum height; in fact, this analysis predicts that the amplitude will increase indefinitely, as shown by (22). However, the concepts and analysis presented in the preceding sections provide a useful framework for discussion of some of the factors determining the heights of fully-developed bed features.

The steepening of antidunes as they grow is no doubt an important factor controlling their height. As antidunes become steeper, the weight of the particles opposes the forward motion of the sediment on the upstream slopes and aids it on the downstream slopes This causes the particles to deposit more readily as the velocity decreases on the upstream slopes, thereby reducing δ, and when the antidunes become steep enough, the deposition all occurs on the upstream slopes and none on the crests. The steepening assists entrainment of particles on the downstream slopes, and a stage is finally reached where the flow picks up such a heavy sediment load on these slopes that no scour occurs in the troughs. When this condition of no deposition at the crests and no scour in the troughs is attained, the antidunes, and also the surface waves, stop growing. Then at the equilibrium height, $\delta = 0$; i.e. there is no lag between changes in velocity and sediment transport. If $\delta = 0$, (22) shows that the linearized analysis predicts no amplitude growth. It also follows from physical reasoning that if there is no lag between velocity and sediment transport changes, no further growth is possible if the features are symmetric. Note that having $\delta = 0$ when the features attain their maximum height does not contradict the notion that it is the value of δ that in part determines the wavelength. It is the value of δ that prevails when the antidunes first start to form that is instrumental in determining their wavelength. The equilibrium heights of sand ripples in the desert have been explained by Kármán (1947) in a similar way. According to Kármán, ripples reach their equilibrium height when the Bernoulli effect, which causes the velocity and sediment transport rate to be greater at the crests and smaller in the troughs, is

just balanced by the gravity effect on the heavy air-sand mixure near the bed; this latter effect causes the velocity and sediment transport to be greater in the troughs and less over the crests.

The factors governing the maximum heights of dunes under a free-surface flow are not so obvious. As dunes become higher, the velocity and shear stress over the crests increase and finally become so high that no further deposition on the crests, and hence no further dune growth, is possible. Similarly, the velocity in the troughs decreases until no further net scour occurs in these regions. When dunes attain their maximum height and move downstream unchanged in form, δ must equal L; otherwise there would be a systematic change in the dune amplitude. Note that if $\delta = L, jkd = 2\pi$ and (22) shows that the linearized formulation predicts no amplitude growth. It seems reasonable that δ might increase as the dunes become higher and steeper because particles leaving the crests have farther to settle to the bed, and are therefore carried a greater distance by the flow before they reach the bed. In addition, the perturbation of the boundary layer and bed shear stress increases as the dunes become higher, probably causing a further increase in δ.

Antidunes frequently become so high before reaching their maximum height governed by the transport of bed material discussed previously that the surface waves above them become unstable and break. The upstream wave in figure 3 is at incipient breaking. There are two different mechanisms that could cause this breaking. The first is separation on the upstream slopes. As the antidunes become higher, the adverse pressure gradient on the upstream slopes increases and might become so great that separation occurs. The separation would upset the flow pattern and precipitate breaking of the waves. The other possible explanation is that the surface waves become so high they reach the maximum amplitude for stability and break. As shown in figure 9, the velocity-wavelength relation for flow over antidunes is not greatly different from that given by (23) for simple deep-water waves. Accordingly the perturbation velocities associated with flow over antidunes are practically the same as the perturbation velocities above an intermediate streamline (which represents the bed) of a stationary deep-water wave in a moving fluid. The profile of deep-water waves has been investigated by Michell (1893) who found that their maximum steepness, $2A_c/L$, is given by

$$2A_c/L = 0{\cdot}142. \tag{33}$$

Twelve observations of the steepness at incipient breaking of long-crested stationary waves above antidunes have been reported by Kennedy (1961*a*). The values ranged from 0·13 to 0·16 and are in good agreement with (33). These measurements indicate that whatever the mechanism actually responsible for the breaking, long-crested waves over antidunes have a maximum steepness that does not differ greatly from the value given by Michell.

7. Concluding remarks

The greatest difficulty encountered in measuring or analyzing dunes is that no two are alike in size or shape, and their spacing is somewhat random, as can be seen in figure 1. When dunes start to form on an initially flat bed (by reducing

the velocity, say, to change from the flat bed to the dune régime) they are long-crested and evenly spaced. Before they reach their maximum height, a segment of a dune will start to move faster than its adjoining parts, and will break away from the original two-dimensional dune. Since each dune is influenced by the characteristics and relative positions of surrounding dunes, soon after one long-crested dune breaks up into three-dimensional features, adjacent ones will also lose their two-dimensional form. The bed configuration soon becomes chaotic and loses any semblance of order except in the statistical sense. The flow separation immediately downstream from each dune and other real-fluid effects such as turbulence and the boundary shear—the very agents responsible for the sediment movement—further complicate the analysis. The principal deficiency of the model developed here when applied to dunes is that it does not adequately take account of these factors. Flow separation was accounted for only by assuming the form of the free streamline (see figure 5), an over-simplified two-dimensional bed profile was used, and a rather unsophisticated transport relation was introduced into the analysis. However, the model does represent the mechanism of dune formation and movement reasonably well, and is adequate for studying their behaviour and many of their characteristics. The model is a much better representation for flow over antidunes since they do have a nearly sinusoidal profile and do not produce flow separation, except perhaps just before the surface waves break.

Some experimental research would appear to be in order now to investigate the quantity δ and its relation to depth and velocity of flow, fluid and sediment properties, and concentration of sediment in the fluid. In fact, to the knowledge of the author, the existence of a lag between the local velocity and local transport rate has not been definitely established. With a better understanding of δ, it would be possible to predict the bed form that will accompany a given flow over a certain bed material, and possibly even the maximum height of the bed features. This would be a big step forward toward being able to predict the roughness of alluvial streams.

Anderson (1953) has also presented an analysis of dunes that is based on the continuity of sediment movement and a potential solution for flow over a wavy bed of variable amplitude. His analysis yielded the following relation:

$$F^2 = \frac{\sinh 2kd}{kd(\tanh kd \sinh 2kd - 2)}.$$

This expression is not greatly different from (27) (the limiting case $j = 0$) for values of kd greater than about 5. For smaller kd, it yields significantly higher Froude numbers.

The general method used here to analyse flow over a bed whose geometry is formed by the flow should be applicable to other problems in which there is an interaction between a moving fluid and its boundaries. For example, a similar analysis might be applied to the formation of dunes in ice by wind, or the formation of dune-like features by a moving fluid that reacts chemically with its boundaries. In the first of these cases, a relation between the local velocity and local heat transfer rate, in which the local heat transfer lags the local velocity,

would have to be formulated. The chemical reaction problem would require a relation between the local velocity and local reaction rate that includes a lag between the local reaction rate and velocity.

In searching the literature for data on bed configurations, it was found that very few authors have given complete, detailed measurements and descriptions of the bed forms of their experiments. Most experimental programmes have been primarily concerned with the roughness and sediment transport of alluvial streams, and it appeared that data on the bed configuration were taken only as a by-product, if at all. It is admittedly difficult and tedious to obtain good bed-form data because of the randomness of the bed features and their unsteady nature. However, the form of the bed plays a large role in determining the roughness of the stream; moreover, since the bed is the source of the transported material and the region of entrainment, the sediment transport rate is no doubt intimately related to the bed geometry. Accordingly, good data on the bed features are as important to the understanding of alluvial streams as data on the sediment transport rate and friction factor—indeed, an analysis of the latter two cannot be logically divorced from the bed configuration—and future workers in this area, both in laboratories and in the field, are urged to make careful measurements and observations of the bed configurations of their streams.

In summary, an analysis of the mechanics of dunes, flat bed, and antidunes formed by a flowing fluid with a free surface has been presented. A mathematical model of free-surface flow over an erodible bed was developed and used to investigate the characteristics of the various bed features and their behaviour. It was found that the type of bed form and wavelength of the bed features depend on the Froude number, the depth of the flow, and the distance δ by which the local sediment transport rate lags the local velocity; the velocity of the bed features was found to depend on these quantities and also the sediment transport rate. The sequence of bed features with increasing velocity predicted by the model is dunes, a régime of transition from dunes to flat bed (in which the bed configuration is not completely described), flat bed, antidunes moving downstream, and antidunes moving upstream. It was found that for large values of δ, the flat bed occurs only over a narrow range of Froude number, and for small δ antidunes moving downstream do not occur. The conditions for the change from one configuration to another were predicted from the model, and equations were derived for the wavelength and velocity of the bed features. Insofar as comparison was possible, good agreement was found between predicted and observed wavelengths of antidunes and ranges of wavelengths of dunes, and values of Froude number at the transition from one bed form to another. Finally, a qualitative discussion of the factors involved in limiting the heights of the bed features was presented.

This theoretical work was supported by the National Institutes of Health, U.S. Public Health Service. It is a sequel to earlier experimental and theoretical work (Kennedy 1961*a*) sponsored by the Agricultural Research Service of the U.S. Department of Agriculture. The many helpful suggestions and criticisms

of Prof. Vito A. Vanoni and Norman H. Brooks, and Mr Robert C. Y. Koh are gratefully acknowledged. The writer is also indebted to Mrs Shirley Graham and Mr Arthur Schmitt for their assistance in preparing the manuscript.

REFERENCES

ANDERSON, ALVIN, G. 1953 The characteristics of sediment waves formed by flow in open channels. *Proc. Third Mid-Western Conf. on Fluid Mech.* University of Minnesota, pp. 379–95.

BARTON, J. R. & LIN, P.-N. 1955 A study of sediment transport in alluvial channels. *Rep. no.* 55JRB2, *Civil Engineering Dep., Colorado A. and M. College.* Ft. Collins, Colorado.

BROOKE BENJAMIN, T. 1957 Wave formation in laminar flow down an inclined plate. *J. Fluid Mech.* **2**, 554–74.

BROOKE BENJAMIN, T. 1959 Shearing flow over a wavy boundary. *J. Fluid Mech.* **6**, 161–205.

BROOKS, N. H. 1954 Laboratory studies of the mechanics of streams flowing over a movable bed of fine sand. Doctoral Thesis, California Institute of Technology.

COLBY, B. R. 1957 Relationship of unmeasured sediment discharge to mean velocity. *Trans. Amer. Geophys. Un.* **38**, 708–17.

COLBY, B. R. 1961 Effect of depth of flow on discharge of bed material. *Geological Survey Water-Supply Paper* 1498-D. U.S. Government Printing Office.

FUCHS, R. A. 1952 On the theory of short-crested oscillatory waves. *Gravity Waves, Nat. Bureau of Standards Circular*, no. 521, pp. 187–200. U.S. Government Printing Office.

GILBERT, G. K. 1914 The transportation of debris by running water. *Geological Survey Water-Supply Paper*, no. 86. U.S. Government Printing Office.

KÁRMÁN, TH. VON 1947 Sand ripples in the desert. *Technion Year Book*, 1947. (Also in *Collected Works of T. von Kármán*, vol. IV, pp. 352–6. London: Butterworths 1956.)

KENNEDY, J. F. 1961*a* Stationary waves and antidunes in alluvial channels. *Rep.* no. KH-R-2, *W. M. Keck Laboratory of Hydraulics and Water Resources, California Institute of Technology.*

KENNEDY, J. F. 1961*b* Further laboratory studies of the roughness and suspended load of alluvial streams. *Rep.* no. KH-R-3, *W. M. Keck Laboratory of Hydraulics and Water Resources, California Institute of Technology.*

LAURSEN, E. M. 1958 The total sediment load of streams. *Proc. Am. Soc. Civ. Engrs, J. Hyd. Div.*, **84**, HY 1, pp. 1530–1 to 1530–36.

MICHELL, J. H. 1893 The highest waves in water. *Phil. Mag.* **36**, 430–7.

MILNE-THOMSON, L. M. 1960 *Theoretical Hydrodynamics.* New York: MacMillan.

PLATE, E. J. O. F. 1957 Laboratory studies on the beginning of sediment ripple formation in an alluvial channel. Masters Thesis, Colorado State University.

SIMONS, D. B., RICHARDSON, E. V. & ALBERTSON, M. L. 1961 Flume studies using medium sand (0·45 mm). *Geological Survey Water-Supply Paper*, no. 1498-A. U.S. Government Printing Office.

SIMONS, D. B. & RICHARDSON, E. V. 1961 Forms of bed roughness in alluvial channels. *Proc. Am. Soc. Civ. Engrs, J. of Hyd. Div.*, **87**, HY 3, 87–106.

SUNDBORG, A. 1957 The river Klarälven; a study in fluvial processes. *Bull.* no. 52, *Institution of Hydraulics, Royal Institute of Technology, Stockholm.*

TISON, L. H. 1949 Origine des ondes de sable et des bancs de sable sous l'action des courants. *Trans. Int. Ass. for Hyd. Structures Research*, Third Meeting, Grenoble.

TSUBAKI, T., KAWASUMI, T. & YASUTOMI, T. 1953 On the influence of sand ripples upon the sediment transport in open channels. *Rep. Res. Inst. for Appl. Mech., Kyushu University*, **2**, 241–56.

VANONI, V. A. & BROOKS, N. H. 1957 Laboratory studies of the roughness and suspended load of alluvial streams. *Rep.* no. E-68, *Sedimentation Laboratory, California Institute of Technology.*

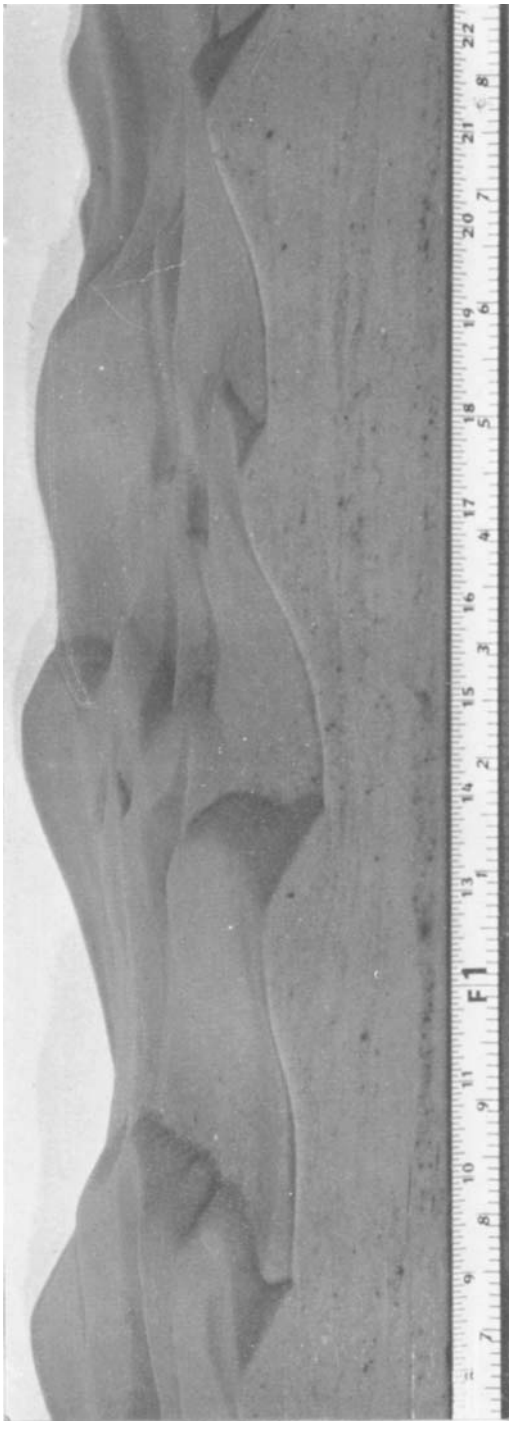

FIGURE 1. Typical dune configuration formed by water flowing over a sand bed in a laboratory flume. The flow is from left to right. Flow velocity = 22·1 cm/sec; water depth = 7·50 cm; average wavelength = 17·4 cm; mean sand size = 0·22 mm. The flume is 26·7 cm wide. (The scale is graduated in feet and tenths, and in inches.)

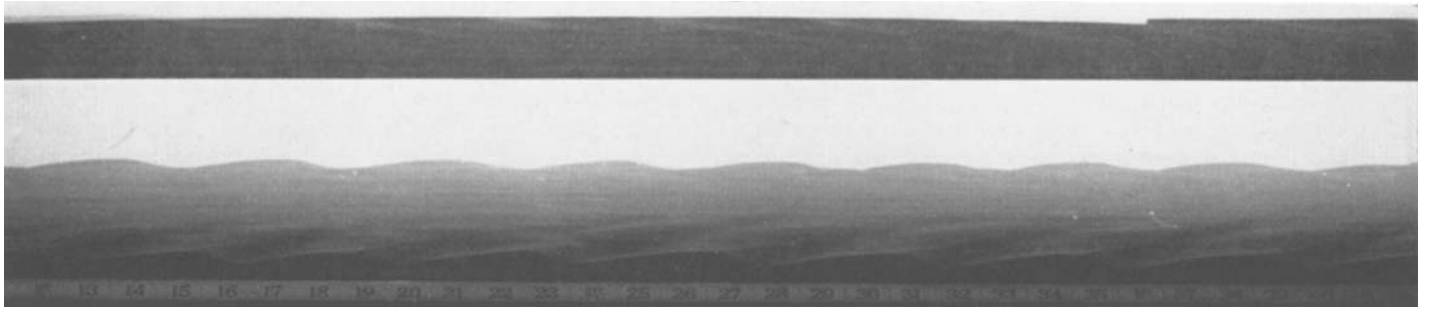

FIGURE 2. Flat-bed configuration formed by water flowing over sand in a laboratory flume. The water is flowing from left to right. The small dunes in the foreground and background are due to the lower local velocities near the flume walls. Flow velocity = 65·0 cm/sec; water depth = 8·55 cm; mean sand size = 0·088 mm. The flume is 26·7 cm wide. (The scale is graduated in inches. Photo.: Brooks 1954.)

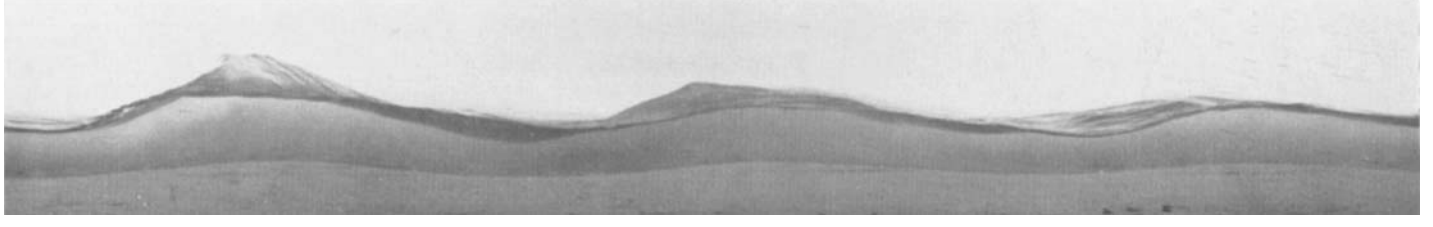

FIGURE 3. Typical antidune configuration generated by a flow of water over a sand bed in a laboratory flume. The flow is from left to right. Note that the wave at the left is at incipient breaking. Flow velocity = 77·8 cm/sec; water depth = 4·52 cm; wavelength = 54·0 cm; mean sand size = 0·233 mm.